AEM
Journals.ASM.org

Iron Transformations Induced by an Acid-Tolerant *Desulfosporosinus* Species

Doug Bertel, John Peck, Thomas J. Quick, and John M. Senko

Department of Geology and Environmental Science, The University of Akron, Akron, Ohio, USA

The mineralogical transformations of Fe phases induced by an acid-tolerant, Fe(III)- and sulfate-reducing bacterium, *Desulfosporosinus* sp. strain GBSRB4.2 were evaluated under geochemical conditions associated with acid mine drainage-impacted systems (i.e., low pH and high Fe concentrations). X-ray powder diffractometry coupled with magnetic analysis by first-order reversal curve diagrams were used to evaluate mineral phases produced by GBSRB4.2 in media containing different ratios of Fe(II) and Fe(III). In medium containing Fe predominately in the +II oxidation state, ferrimagnetic, single-domain greigite (Fe_3S_4) was formed, but the addition of Fe(III) inhibited greigite formation. In media that contained abundant Fe(III) [as schwertmannite; $Fe_8O_8(OH)_6SO_4 \cdot nH_2O$], the activities of strain GBSRB4.2 enhanced the transformation of schwertmannite to goethite (α-FeOOH), due to the increased pH and Fe(II) concentrations that resulted from the activities of GBSRB4.2.

Coal mine-associated acid mine drainage (AMD) is produced when oxygenated water comes in contact with pyrite (FeS_2) or other iron sulfide minerals that are exposed during the mining process (2). The sulfide moiety of iron sulfides (mostly pyrite; FeS_2) is oxidized via microbiological activities, yielding fluids with low pH (generally ranging from pH 2.5 to 4.5) and high dissolved Fe(II) and sulfate concentrations. Intrusion of these acidic and Fe-rich fluids into surface waters often results in waterways that are largely devoid of macrofauna and -flora, as the stream beds are covered by Fe(III) (hydr)oxide phases (26). The primary and most challenging goal of AMD attenuation is to remove dissolved Fe from solution before the AMD reaches these surface waters.

A recently proposed strategy for removal of dissolved Fe from AMD is to exploit the activities of Fe(II)-oxidizing bacteria (FeOB) in "iron mounds" that result when AMD flows as a 0.5- to 1-cm sheet over the terrestrial surface (16, 59). The "sheet flow" characteristic of the AMD facilitates aeration of the fluids, enhancing the activities of FeOB. The Fe(III) that results from FeOB activities subsequently precipitates from solution, giving rise to iron mounds, which are composed almost exclusively of Fe(III) (hydr)oxide phases and may reach depths of tens to hundreds of centimeters (59) and in which Fe may be sequestered before it reaches surface waters. However, as Fe(III) (hydr)oxide phases accumulate, diffusion of O_2 into the sediments may be limited, giving rise to anoxic regions of the iron mound, and enhancing anaerobic activities at depths within the iron mound (21, 36, 41, 45).

While anaerobic microbial activities (notably sulfate reduction) have been exploited for AMD remediation (4, 8, 22, 27), in the context of iron mound systems, they may be considered detrimental to the overall goal of oxidatively precipitating Fe and maintaining the Fe(III) (hydr)oxide precipitates. The most abundant anaerobic terminal electron acceptors in AMD-impacted systems are sulfate and the Fe(III) (hydr)oxides. Anaerobic activities in iron mounds may lead to the reductive dissolution of Fe(III) (hydr)oxides via the direct, enzymatic reduction of Fe(III) by Fe(III)-reducing bacteria (FeRB) (equation 1) or by reaction with sulfide produced by sulfate-reducing bacteria (SRB) (equation 2) (17, 46).

$$4Fe(OH)_3 + CH_2O + 8H^+ \rightarrow 4Fe^{2+} + CO_2 + 11H_2O \quad (1)$$

$$2Fe(OH)_3 + S^{2-} + 4H^+ \rightarrow 2Fe^{2+} + S + 6H_2O \quad (2)$$

SRB activities may also lead to the concentration of iron sulfide species at the terrestrial surface, in closer proximity to atmospheric O_2, and pose a greater risk of acid production should O_2 infiltrate the sediments (22, 28).

Anaerobic activities associated with AMD-impacted systems remain somewhat nebulous. For instance, most cultured acidophilic FeRB reduce Fe(III) optimally in the presence of O_2 (13). SRB activity in AMD-impacted systems is well documented (e.g., 4, 14, 21, 22, 27), but given the abundance of sulfate in these systems, surprisingly few acidophilic or acid-tolerant SRB have been recovered in culture (29). Strictly anaerobic SRB that have been isolated from AMD-impacted systems fall into the genus *Desulfosporosinus* (1, 29, 33, 60), and representatives of this genus are frequently detected in anoxic regions of AMD-impacted systems (7, 23, 32, 55, 68). As such, *Desulfosporosinus* spp. may play an important role in modulating the biogeochemical cycling of Fe and S (e.g., equations 1 and 2) in AMD-impacted systems where anoxic conditions are encountered.

The geochemical and mineralogical consequences of anaerobic microbial activities [including the formation and identity of FeS phases and transformations of Fe(III) phases] will exert considerable control over the susceptibility of those phases to subsequent microbially mediated redox alteration and the long-term performance of iron mound systems if they are to be implemented as AMD treatment strategies. In the present study, Fe-containing mineralogical products and transformations that were induced by a sulfate- and metal-reducing *Desulfosporosinus* species (GBSRB4.2) (60) were evaluated under conditions associated with

Received 26 July 2011 **Accepted** 23 October 2011
Published ahead of print 28 October 2011
Address correspondence to John M. Senko, senko@uakron.edu.

doi:10.1128/AEM.06337-11

TABLE 1 HCl-extractable Fe(II) and hydroxylamine-HCl-extractable Fe(III) contents of uninoculated media and cultures of *Desulfosporosinus* sp. strain GBSRB4.2 after 24 days of incubation

Anticipated Fe(II):Fe(III) ratio	Mean (SEM) concn (mM) of the indicated form of Fe in:					
	Uninoculated medium			Inoculated medium after 24 days		
	HCl-extractable Fe(II)	Hydroxylamine-HCl-extractable Fe(III)	Total extractable Fe[a]	HCl-extractable Fe(II)	Hydroxylamine-HCl-extractable Fe(III)	Total extractable Fe
1 Fe(II):0 Fe(III)	38 (±2)	1 (±0.4)	39	25 (±1)	1 (±0.7)	26
3 Fe(II):1 Fe(III)	26 (±3)	11 (±3)	37	28 (±5)	6 (±2)	34
1 Fe(II):3 Fe(III)	11 (±2)	30 (±2)	41	11 (±2)	10 (±3)	21
0 Fe(II):1 Fe(III)	0.1 (±0.09)	38 (±1)	38	1 (±0.4)	16 (±5)	17

[a] Total extractable Fe represents the sum of HCl-extractable Fe(II) and hydroxylamine-HCl-extractable Fe(III).

AMD-impacted systems (i.e., initially low pH and high Fe concentrations).

MATERIALS AND METHODS

GBSRB4.2 growth. *Desulfosporosinus* sp. strain GBSRB4.2 is an acid-tolerant, metal-reducing SRB isolated from iron mound sediments that incompletely oxidizes glucose to acetate and CO_2 coupled with sulfate reduction (60). GBSRB4.2 is also capable of oxidizing H_2 and lactate to support growth under sulfate-reducing conditions (60). GBSRB4.2 was routinely grown in a medium containing $FeSO_4$ (40 mM), $(NH_4)_2SO_4$ (10 mM), glucose (5 mM), $MgSO_4$ (2 mM), Trypticase soy broth (0.5 g/liter), vitamins and trace metals (64), and the pH of the medium was adjusted to 4.2 with H_2SO_4 (60). The medium was purged with N_2, sealed, and placed in an anoxic chamber where it was dispensed into serum bottles under an atmosphere of 97% N_2 and 3% H_2. Serum bottles were subsequently sealed in the anoxic chamber, so the headspace of the bottles contained the same gas composition as the chamber. For experiments to examine the effect of Fe oxidation state on the formation and transformation of Fe phases, strain GBSRB4.2 was cultured in the medium described above, with iron sulfate provided as either $FeSO_4$ or $Fe_2(SO_4)_3$. For the types of media containing Fe(II), $FeSO_4$ was added to media from an anoxic, filter-sterilized stock solution (400 mM) to achieve the desired Fe(II) concentrations. For the types of media containing Fe(III), $Fe_2(SO_4)_3$ was added from a stock suspension (130 mM) in which the pH was adjusted to 4.0 with NaOH, resulting in an orange/brown Fe(III) (hydr)oxide precipitate. Iron sulfates were added to media to achieve anticipated Fe(II):Fe(III) ratios of 1 Fe(II):0 Fe(III), 3 Fe(II):1 Fe(III), 1 Fe(II):3 Fe(III), and 0 Fe(II):1 Fe(III), each with a total Fe concentration of 40 mM. Addition of $FeSO_4$ and/or $Fe_2(SO_4)_3$ to the different media resulted in sulfate concentrations of 40 mM, 45 mM, 55 mM, and 60 mM in media amended with Fe at Fe(II):Fe(III) ratios of 1 Fe(II):0 Fe(III), 3 Fe(II):1 Fe(III), 1 Fe(II):3 Fe(III), and 0 Fe(II):1 Fe(III), respectively. All cultures were incubated at approximately 25°C, and uninoculated media served as negative controls. Samples were periodically removed from cultures in an anoxic glove bag and analyzed as described below.

Analytical techniques. To measure the pH of cultures, the samples were placed in microcentrifuge tubes and removed from the glove bag, and the pH was immediately measured. For sulfide analysis, 0.1 ml of sample was preserved in 0.4 ml of 10% zinc acetate (anoxic) and subsequently quantified using the methylene blue assay (12). Fe(II) and Fe(III) were extracted from solids using 0.5 M HCl and 0.25 M hydroxylamine in 0.25 M HCl, respectively (35). In Fe(II) and Fe(III) extractions, solids were separated from the soluble fraction by centrifugation, and Fe(II) in the supernatant was quantified by the ferrozine assay (63).

Characterization of Fe phases. When GBSRB4.2 cells had reached the stationary phase of growth (24 days), the cells and associated Fe-containing solid phases were harvested by centrifugation, dried under anoxic conditions, and characterized by powder X-ray powder diffraction (XRD) analysis and magnetometry. Samples for XRD were placed in low-background quartz mounting disks, and analysis was carried out using a Phillips 3100 automated diffractometer using CuKα radiation scanning at 2Θ of 2° to 70°, with an accelerating voltage of 40 kV at 35 mA. Intensities were measured with a 0.02° step size and 1-s counting time per step. Sample spectra were then compared to reference spectra to identify mineral phases.

The magnetic hysteresis properties of the Fe-containing phases were analyzed using an alternating gradient magnetometer (AGM) (Princeton Measurements Corp., Princeton, NJ). Samples were mounted to the AGM probe using silicone grease that is weakly diamagnetic and is easily negated by the sample's stronger ferrimagnetic properties. Initial sample demagnetization was followed by application of a weak field (roughly 25 mT), allowing for measurement of the initial slope (IS). IS roughly mimics the magnetic susceptibility (χ), or how receptive a material is to a magnetic field. Next, the magnetic field was increased stepwise to ±1.4 T to measure a hysteresis loop, providing values for saturation magnetization (M_s; the point at which the sample was magnetically saturated), saturation remanent magnetization (M_{rs}; the magnetic saturation memory held by the sample upon removal of the field), and magnetic coercivity (H_c; the field needed to return a sample magnetization to zero while in a magnetic field). The samples were then demagnetized and exposed to another field to measure the acquisition of the isothermal remnant magnetization (IRM) of the sample. In this procedure, a positive field was applied to a sample in 100-mT increments up to 500 mT, until remanent magnetization had been achieved. The magnetic remanent coercivity (H_{rc}; the field needed to completely remove the sample magnetization upon removal of the field) was measured by applying and removing a negative field in stops until remanent magnetization (M_r) reached zero. Finally, 121 individual partial hysteresis loops were measured. These loops were then used to create a first-order reversal curve (FORC) diagram, using FORCOBELLO MATLAB code version 0.99c (69). A smoothing function of 2 was used on all samples to build the FORC diagrams. FORC diagrams have the advantage over major hysteresis loops in that they can better differentiate the coercivity distribution within a sample. FORC diagrams also show the degree of magnetic interaction between grains within a sample. Samples were not mass normalized, since they were powdery and very small.

RESULTS

Growth and activities of *Desulfosporosinus* sp. strain GBSRB4.2 with different Fe(II):Fe(III) ratios. Extraction of Fe from the uninoculated media [containing various ratios of Fe(II):Fe(III)] using 0.5 M HCl and 0.25 M hydroxylamine-HCl in 0.25 M HCl [for Fe(II) and Fe(III), respectively] revealed a small amount of Fe(III) in the medium amended with $FeSO_4$ [but no additional Fe(III)], likely due to a minor amount of Fe(II) oxidation during solution preparation (Table 1). When iron and sulfate were provided as $Fe_2(SO_4)_3$ [media containing 3 Fe(II):1 Fe(III), 1 Fe(II):3 Fe(III), and 0 Fe(II):1 Fe(III)], Fe(III) (hydr)oxide precipitates formed that were susceptible to reductive dissolution by hydroxylamine-HCl (Table 1). Relatively crystalline Fe(III) (hydr)oxide phases

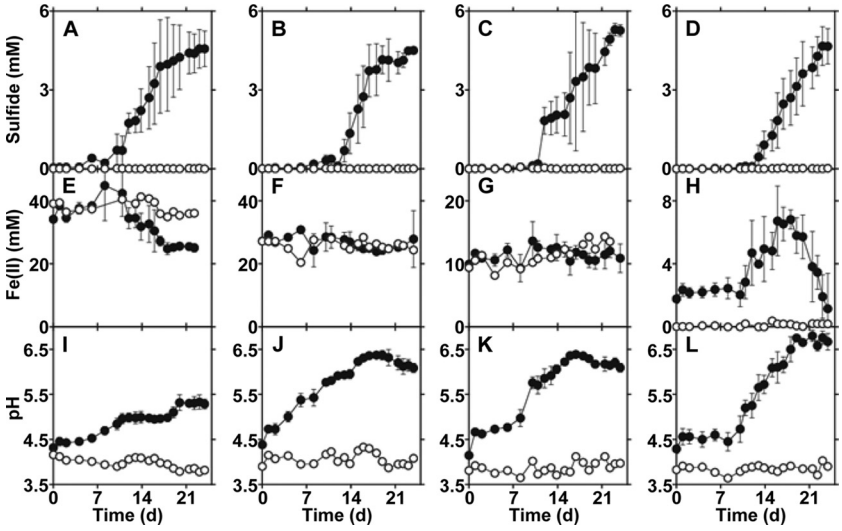

FIG 1 (A to L) Sulfide concentrations, 0.5 M HCl-extractable Fe(II) concentrations, and pH in uninoculated media (○) and cultures of GBSRB4.2 (●) containing anticipated Fe(II):Fe(III) ratios of 1 Fe(II):0 Fe(III) (A, E, and I), 3 Fe(II):1 Fe(III) (B, F, and J), 1 Fe(II):3 Fe(III) (C, G, and K), and 0 Fe(II):1 Fe(III) (D, H, and L). The *y* axes show time (in days). Each value is the mean ± 1 standard deviation (error bar).

(e.g., goethite or hematite) are generally resistant to reduction in hydroxylamine-HCl (35), but the results presented here suggest that Fe(III) phases in the growth media were susceptible to nearly complete reduction, due to smaller grain size and/or the poor crystallinity of the Fe(III) (hydr)oxide phases (e.g., ferrihydrite or schwertmannite). Total extractable Fe (the sum of HCl- and hydroxylamine-HCl-extractable Fe) ranged from 37 to 41 mM, and the desired Fe(II):Fe(III) ratios were generally achieved (Table 1).

Sulfide accumulated to a concentration of approximately 5 mM in all media inoculated with strain GBSRB4.2, regardless of Fe(II):Fe(III) ratio, and no sulfidogenesis occurred in uninoculated controls (Fig. 1A to D). In cultures amended with 0 Fe(II):1 Fe(III), Fe(II) accumulation preceded sulfidogenesis (Fig. 1D), suggesting that Fe(III) reduction partially occurred independently of sulfate reduction (i.e., enzymatically). It is also notable that the presence of Fe(III) [i.e., media amended with 3 Fe(II):1 Fe(III), 1 Fe(II):3 Fe(III), and 0 Fe(II):1 Fe(III)] appeared to delay the onset of sulfidogenesis in comparison to medium amended with 1 Fe(II):0 Fe(III) (Fig. 1A to D), suggesting that Fe(III) may partially serve as a competitive electron acceptor with sulfate. However, with continued incubation in medium amended with 0 Fe(II):1 Fe(III), sulfate and Fe(III) reduction occurred concurrently (Fig. 1D), suggesting that the presence of Fe(III) does not completely inhibit sulfate reduction by GBSRB4.2, despite the ability of GBSRB4.2 to reduce Fe(III) (hydr)oxides enzymatically (60).

The pH of all GBSRB4.2 cultures increased over a period of 23 days, and no change in pH was observed in uninoculated controls (Fig. 1I to L). The increase in pH of these cultures is attributable to (i) consumption of protons associated with Fe(III) (hydr)oxide reduction (equations 1 and 2), (ii) the conversion (equation 3) of strongly acidic sulfate ($H_2SO_4 \leftrightarrow HSO_4^-$, $pK_a = -3.0$, $HSO_4^- \leftrightarrow SO_4^{2-}$, $pK_a = 1.99$) to weakly acidic sulfide ($H_2S \leftrightarrow HS^-$, $pK_a = 6.9$, $HS^- \leftrightarrow S^{2-}$, $pK_a = 14$), and (iii) increased alkalinity associated with oxidation of organic carbon to CO_2 (60).

$$SO_4^{2-} + 2CH_2O + H^+ \rightarrow HS^- + 2CO_2 + 2H_2O \quad (3)$$

After 24 days of growth, the pH of cultures containing 1 Fe(II):0 Fe(III) was approximately 5.5 (Fig. 1I), while the pH of cultures containing 3 Fe(II):1 Fe(III), 1 Fe(II):3 Fe(III), and 0 Fe(II):1 Fe(III) had increased to approximately 6.5 (Fig. 1J to L), likely due to the influence of Fe(III) reduction on the pH of the media (equations 1 and 2).

HCl-extractable Fe(II) concentration in cultures amended with 1 Fe(II):0 Fe(III) decreased concurrently with sulfidogenesis (Fig. 1A and E), and HCl-extractable Fe(II) concentrations remained constant in cultures amended with 3 Fe(II):1 Fe(III) and 1 Fe(II):3 Fe(III) (Fig. 1F and G). In cultures amended with 0 Fe(II):1 Fe(III), an initial increase in HCl-extractable Fe(II) concentration occurred, followed by a decrease in HCl-extractable Fe(II) with continued incubation (Fig. 1H). No change in Fe(II) concentration was detected in the uninoculated media (Fig. 1E to H). The decrease in HCl-extractable Fe(II) in cultures amended with 1 Fe(II):0 Fe(III), lack of increase in HCl-extractable Fe(II) concentrations in cultures amended with 3 Fe(II):1 Fe(III) and 1 Fe(II):3 Fe(III), and decrease in HCl-extractable Fe(II) concentrations in cultures amended with 0 Fe(II):1 Fe(III) is somewhat surprising, since strain GBSRB4.2 appeared to initially reduce Fe(III) independently of sulfidogenesis (Fig. 1H), and sulfide was produced in all cultures, which presumably would have reduced Fe(III) to Fe(II) (17, 46). Indeed, black precipitates were observed in all cultures, suggesting the formation of FeS phases. The lack of HCl-extractable Fe(II) in the cultures suggested the formation of FeS phases that were resistant to dissolution by 0.5 M HCl (e.g., pyrrhotite [$Fe_{1-x}S$, where $0 < x < 0.2$], greigite [Fe_3S_4], marcasite [FeS_2], or pyrite [50, 61]). In cultures amended with 1 Fe(II):3 Fe(III) and 0 Fe(II):1 Fe(III), a decrease in hydroxylamine-HCl-extractable Fe(III) was observed (Table 1), suggesting that activities of GBSRB4.2 induced a transformation of Fe(III) (hydr)oxides to Fe(III) phases that were resistant to reduction by hydroxylamine.

Solid-phase characterizations. After 24 days of incubation, the solid phases in the uninoculated media and GBSRB4.2 cul-

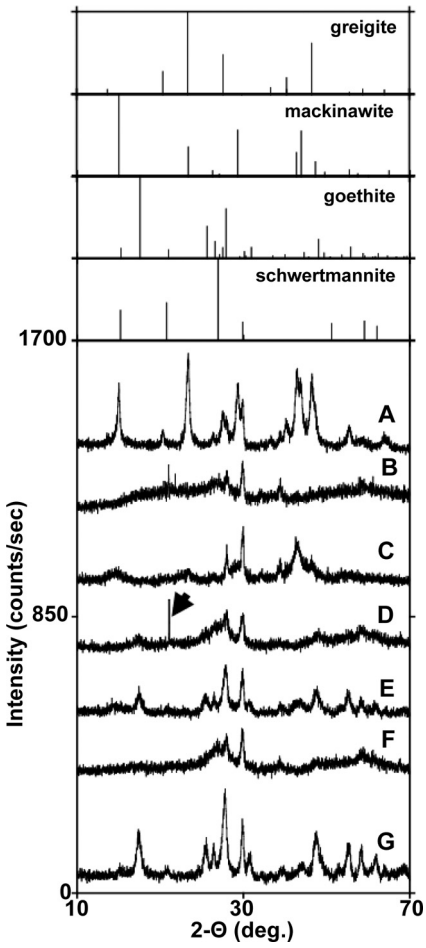

FIG 2 X-ray diffraction spectra of the solid phases recovered from GBSRB4.2 culture containing 1 Fe(II):0 Fe(III) (A), uninoculated medium and GBSRB4.2 culture containing 3 Fe(II):1 Fe(III) (B and C, respectively), uninoculated medium and GBSRB4.2 culture containing 1 Fe(II):3 Fe(III) (D and E, respectively), uninoculated medium and GBSRB4.2 culture containing 0 Fe(II):1 Fe(III) (F and G, respectively). A quartz signal attributable to the sample mounting slide is indicated by the black arrow in XRD spectrum D. Data used to construct the reference spectra of greigite, mackinawite, goethite, and schwertmannite are from The American Mineralogist Crystal Structure Database (18).

tures were dried in an anoxic environment and characterized by XRD and magnetometry. Analysis of the solid phases from uninoculated media by XRD suggested that the predominant mineral in all cases was schwertmannite (Fig. 2B, D, and F), a poorly ordered Fe(III) (hydr)oxysulfate [general formula $Fe_8O_8(OH)_6SO_4 \cdot nH_2O$] that is often encountered in AMD-impacted systems (5, 6, 58). XRD analysis of the solid phases recovered from the GBSRB4.2 cultures that were amended with 1 Fe(II):0 Fe(III) suggested the presence of mackinawite (FeS) and greigite (Fe_3S_4), a ferrimagnetic FeS phase (Fig. 2A) (50). Cultures amended with 3 Fe(II):1 Fe(III) also contained mackinawite and greigite, but the spectrum had broader, less defined peaks, suggesting that these FeS phases were poorly crystalline in comparison to those observed in the cultures amended with 1 Fe(II):0 Fe(III) (Fig. 2A and C). In cultures containing 1 Fe(II):3 Fe(III) and 0 Fe(II):1 Fe(III), the predominant mineral phase identified by XRD was goethite, with minor mackinawite peaks (Fig. 2E and G), suggesting that the activities of GBSRB4.2 enhanced the transformation of schwertmannite to goethite.

To evaluate the magnetic characteristics of the solid phases in GBSRB4.2 cultures and uninoculated media, first-order reversal curve (FORC) diagrams were constructed for the solid phases recovered from incubations. FORC diagrams of the solid phases in uninoculated media amended with 3 Fe(II):1 Fe(III), 1 Fe(II):3 Fe(III), and 0 Fe(II):1 Fe(III) (identified as schwertmannite by XRD) exhibited high levels of noise typical of weakly magnetic Fe(III) (hydr)oxides (Fig. 3B, D, and F) (20) such as schwertmannite. H_c values determined for FORC diagrams of the solid phases produced in GBSRB4.2 cultures amended with 1 Fe(II):0 Fe(III) and 3 Fe(II):1 Fe(III) were higher than those of cultures amended with 1 Fe(II):3Fe(III) and 0 Fe(II):1Fe(III) (Fig. 3A, C, E, and G). The FORC diagrams of the solid phases recovered from GBSRB4.2 cultures amended with 1 Fe(II):0 Fe(III) and 3 Fe(II):1 Fe(III) exhibited moderately high concentric contours that were similar to FORC diagrams of greigite-bearing sediments (Fig. 3A and C) (51). This FORC pattern suggests single-domain greigite grains (51). These two samples also had the highest M_{rs} and M_s values of all samples measured. Because similar amounts of each sample were analyzed, the higher M_{rs} values confirm the presence of the strongly ferrimagnetic mineral greigite, identified by XRD. With increasing Fe(III) content [i.e., cultures amended with 3 Fe(II):1 Fe(III)], a diminished FORC greigite signal was observed, corresponding to the more poorly crystalline greigite XRD pattern (Fig. 2C). In GBSRB4.2 cultures amended with 1 Fe(II):3 Fe(III) and 0 Fe(II):1 Fe(III), FORC diagrams (Fig. 3E and G) exhibited scatter similar to the respective uninoculated media. Similarly high levels of noise have been reported for goethite (α-FeOOH), and this has been attributed to the high coercivity (H_c) and low-saturation magnetization (M_s) of goethite (51, 54).

A ratio of the M_r values taken at 500 mT and 1.4 T showed that saturation had been achieved in all but one sample (saturation ratio [S-ratio] values of 0.99), suggesting the presence of low-coercivity minerals, such as greigite and schwertmannite. In the sample obtained from the GBSRB4.2 culture amended with 0 Fe(II):1 Fe(III), complete saturation was not achieved (S-ratio value of 0.46), suggesting the presence of a high-coercivity mineral, such as goethite. Goethite generally requires a very high field to fully saturate, due to its high coercivity (20). It was anticipated that magnetic saturation would not be fully achieved in the GBSRB4.2 cultures amended with 1 Fe(II):3 Fe(III) because XRD identified the presence of goethite (Fig. 2E). The critical single-domain size for hematite is 15 μm (19). Since goethite and hematite are weakly magnetic materials, they are likely to have similarly large critical single-domain grain sizes. The grains obtained from the GBSRB4.2 culture amended with 0 Fe(II):1 Fe(III) were roughly 10 to 12 μm as measured by scanning electron microscopy (SEM) (not shown), and thus likely superparamagnetic and not single domain in size. In addition, the minor amount of Fe(II)-bearing minerals (e.g., mackinawite) in the sample and small sample size may have masked the high-coercivity goethite signal.

DISCUSSION

Formation of magnetic FeS phases. SRB activities may yield mackinawite and greigite at circumneutral pH (3, 24, 25, 49), and the current study shows the formation of greigite under geochemical conditions representative of some AMD-impacted systems.

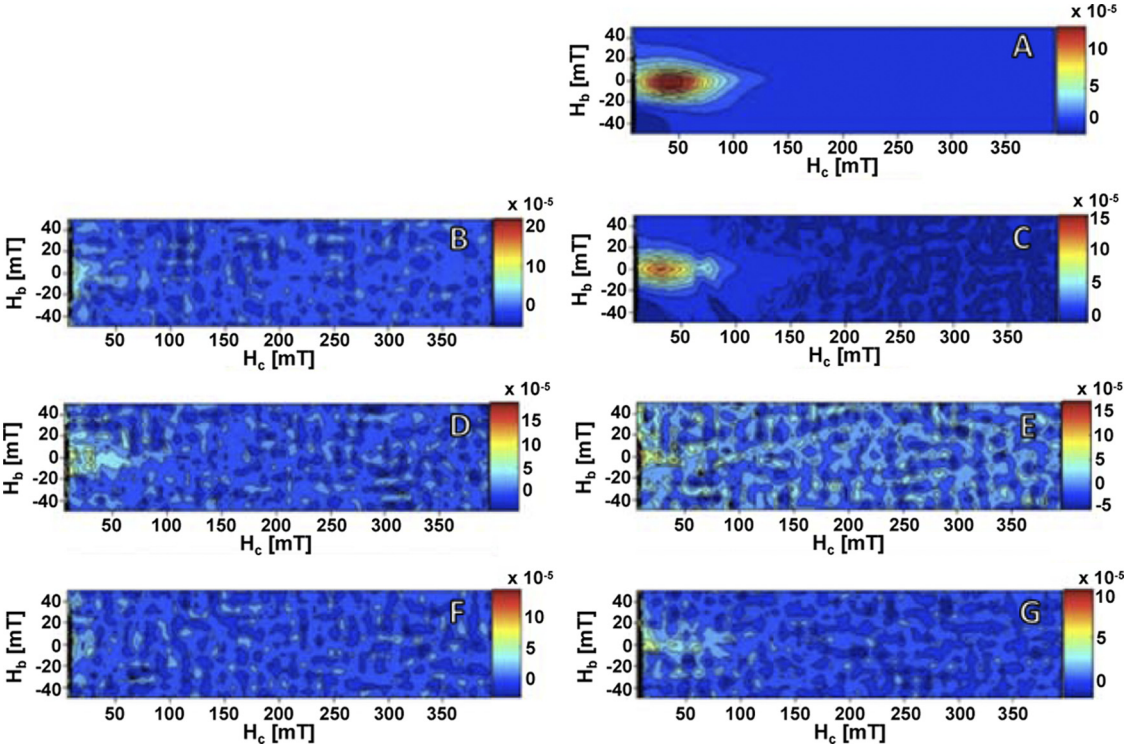

FIG 3 (A to G) FORC diagrams of the solid phases in GBSRB4.2 cultures amended with 1 Fe(II):0 Fe(III) (A), 3 Fe(II):1 Fe(III) (C), 1 Fe(II):3 Fe(III) (E), and 0 Fe(II):1 Fe(III) (G) and uninoculated media amended with 3 Fe(II):1 Fe(III) (B), 1 Fe(II):3 Fe(III) (D), and 0 Fe(II):1 Fe(III) (F).

Greigite appears to form via the maturation of mackinawite, which is metastable with respect to greigite (34, 43, 44, 50, 52, 56). Greigite is more resistant to dissolution than mackinawite under acidic conditions (50, 61), and a decrease in 0.5 M HCl-extractable Fe(II) occurred in GBSRB4.2 cultures amended with 1 Fe(II):0 Fe(III) (Fig. 1A), suggesting that mackinawite was initially formed in the cultures and transformed to greigite with continued incubation. The exact mechanisms of, and optimal conditions for greigite formation from "amorphous" FeS or mackinawite remain unclear (50). Greigite is a Fe(II)- and Fe(III)-containing mineral phase, so it has been suggested that some oxidant [e.g., O_2 or S(0)], is necessary for mackinawite transformation to greigite (34, 44, 50, 52, 56). However, the transformation of mackinawite to greigite has been reported in the absence of oxidant and may be enhanced by low pH and/or excess sulfide (24, 50, 67). While the possibility of mackinawite-Fe(II) oxidation during XRD and magnetic analyses cannot be completely discounted, the samples were dried and stored under O_2-free conditions prior to analysis and were not exposed to air for more than 2 h during these analyses. Low levels of Fe(III) present in greigite-containing cultures (Table 1) may have served as an indirect oxidant to enhance mackinawite transformation to greigite.

While Fe(III) may act as an indirect oxidant and enhance the formation of greigite from mackinawite, the results presented here suggest that abundant Fe(III) inhibits greigite formation. Greigite is a product of SRB activity in the presence of dissolved Fe(II) (24, 25), but pyrrhotite (Fe_7S_8) is the major FeS product of SRB activities in the presence of hematite [Fe(III); α-Fe_2O_3], perhaps due to interactions between sulfide and Fe(III) surfaces (39). Marius et al. (38) found that neutrophilic SRB activity in the presence of Fe(II):Fe(III) ratios of 15 Fe(II):1 Fe(III) yielded FeS phases with higher magnetic susceptibility than lower Fe(II):Fe(III) ratios, though more detailed characterization of the FeS phases was not conducted. The results presented here provide evidence that abundant schwertmannite-Fe(III), which would be expected in some AMD-impacted systems, inhibits the formation of greigite by SRB activity.

Schwertmannite-to-goethite transformation. Activities of the acid-tolerant Fe(III)- and sulfate-reducing bacterium GBSRB4.2 enhanced the transformation of schwertmannite to goethite in media amended with 1 Fe(II):3 Fe(III) and 0 Fe(II):1 Fe(III). GBSRB4.2 has previously been shown to couple H_2 oxidation to the reduction of Fe(III) (hydr)oxides in the absence of sulfate under non-growth conditions (60), and current work is focused on evaluating the ability of GBSRB4.2 to exploit Fe(III) reduction for growth. While *Desulfosporosinus* species have been shown to enzymatically reduce Fe(III), GBSRB4.2 is notable among the acidophilic/acid-tolerant *Desulfosporosinus* species in its ability to reduce metals (1, 33, 47, 53, 62, 65). Previous work illustrated that under conditions approximating the *in situ* chemistry of an iron mound system [abundant Fe(III) and sulfate], GBSRB4.2 reduced Fe(III) and sulfate concurrently under non-growth conditions (60). However, GBSRB4.2 reduced Mn(IV) and U(VI) to the exclusion of sulfate reduction (60), suggesting that concurrent Fe(III) and sulfate reduction was attributable to the similar energetics of Fe(III) and sulfate reduction (Gibbs free energy of the reaction [ΔG°_r] = -75 kJ mol^{-1} and -47 kJ mol^{-1}, respectively; values calculated from reference 15) compared to more thermodynamically favorable electron acceptors Mn(IV) and U(VI) ($\Delta G^\circ_r = -189$ kJ mol^{-1} and -126 kJ mol^{-1}, respec-

tively; values calculated from reference 15). In medium amended with 0 Fe(II):1 Fe(III), initiation of Fe(III) reduction and pH increase preceded sulfidogenesis, but subsequently, the two processes also occurred concurrently (Fig. 1D, H, and L). The onset of sulfidogenesis after incomplete reduction of Fe(III) may be attributable to the formation of goethite, which would likely be more resistant to bioreduction than schwertmannite (9, 10). Taken together, these results suggest that Fe(III) reduction by GBSRB4.2 is a result of enzymatic Fe(III) reduction and reaction of Fe(III) with biogenic sulfide.

GBSRB4.2 appears to mediate two chemical changes that facilitate the transformation of schwertmannite to goethite: (i) production of Fe(II) via enzymatic reduction of Fe(III) and via the reaction of Fe(III) with biogenic sulfide, and (ii) neutralization of acidic fluids. Schwertmannite is metastable with respect to goethite, and the schwertmannite-to-goethite transformation (equation 4, with nH$_2$O neglected) is enhanced by high pH (5, 57).

$$Fe_8O_8(OH)_{8-2x}(SO_4)_x + 2H_2O \rightarrow 8\alpha\text{-FeOOH} + SO_4^{2-} + 2H^+ \quad (4)$$

Under acidic conditions, the transformation of schwertmannite to goethite may occur over periods of several years (5, 30, 40), while at circumneutral pH, the reaction may occur over periods of 100 days (57). Recent work by Burton et al. (10, 11) has suggested that Fe(II) enhances the schwertmannite-to-goethite transformation, with the Fe(II)-enhanced reaction occurring over periods of hours. XRD revealed that schwertmannite was the dominant Fe(III) phase in uninoculated media containing 3 Fe(II):1 Fe(III) and 1 Fe(II):3 Fe(III), and it appears that minimal schwertmannite-to-goethite transformation occurs at pH $<$ 5 (10). The lack of Fe(II)-induced schwertmannite transformation at low pH indicates that the reaction is dependent on Fe(III) phase-associated Fe(II), and at low pH, Fe(II) tends to remain in solution (10). The transformation of schwertmannite to goethite may be enhanced at low sulfate concentrations (31), so SRB activities could enhance this reaction via consumption of sulfate. However, given the sulfate concentrations in the different media (ranging from 40 to 60 mM), the amount of sulfidogenesis (approximately 5 mM) would not lead to significant depletion of sulfate.

It appears that microbially induced transformation of schwertmannite to goethite would not occur without the increased pH that resulted from the Fe(III)- and sulfate-reducing activities of GBSRB4.2 (equations 1, 2, and 3). Subsequently, increased pH facilitated the Fe(II)-enhanced transformation of schwertmannite to goethite. Burton et al. (9, 10) have suggested that FeRB-mediated transformation of schwertmannite to goethite may facilitate the activities of SRB via the formation of a less thermodynamically favorable terminal electron acceptor (TEA) (goethite) than schwertmannite (equations 5 and 6; goethite and schwertmannite Gibbs free energy of formation [ΔG°_f] from reference 37; All other ΔG°_f values are from reference 15).

$$H_2 + 2\alpha\text{-FeOOH} + 4H^+ \rightarrow 2Fe^{2+} + 4H_2O \quad (5)$$

$$H_2 + 0.25Fe_8O_8(OH)_6SO_4 + 3.5H^+ \rightarrow 2Fe^{2+} + 0.25SO_4^{2-} + 3.5H_2O \quad (6)$$

For equation 5, ΔG°_r equals -39 kJ/mol H$_2$, while for equation 6, ΔG°_r equals -62 kJ/mol H$_2$. Under this scenario, when schwertmannite is abundant, FeRB are able to couple oxidation of electron donors with schwertmannite-Fe(III) reduction to the exclusion of SRB activities. With the increase in pH and Fe(II) that accompany FeRB activities (equation 3), a schwertmannite-to-goethite transformation is induced. Subsequently, the poor bioreducibility of goethite facilitates SRB activity (9, 10). This has been supported by depth- and E_h-dependent transitions within sediments from schwertmannite-rich material in upper regions of sediment columns and goethite-rich material in lower, more-reducing regions (9, 10). Indeed, in these studies, goethite and FeS phases (identified as mackinawite) were colocalized within the sediment columns (9). The work presented here supports this hypothesis and also suggests that SRB activities are not only facilitated by the schwertmannite-to-goethite transformation but that the activities of a Fe(III)- and sulfate-reducing bacterium induce the transformation.

Environmental implications. Under conditions representative of AMD (i.e., initially low pH, high Fe concentrations), anaerobic microbial activities [i.e., Fe(III) and sulfate reduction] may lead to two major mineralogical (trans)formations: (i) the formation of the ferrimagnetic mineral phase greigite under conditions of high Fe(II):Fe(III) ratios and (ii) the transformation of schwertmannite to goethite. A goal of anaerobic AMD treatment systems (e.g., anoxic limestone drains) is to minimize Fe(III) formation, while precipitating Fe(II) and other metals as sulfide phases (4, 8, 27, 22). In these Fe(III)-free systems, greigite may be an important product of SRB activities. The magnetic properties of FeS phases resulting from SRB activities may be used as a diagnostic tool to evaluate the performance of anaerobic AMD treatment systems (42) or for the selective recovery of metals (e.g., Cu, Ni, Pb, and Zn) that adsorb strongly to ferrimagnetic FeS phases (66). Furthermore, greigite represents a more stable iron sulfide phase that will be more resistant to oxidation and regeneration of acidity should O_2 be introduced into the sediments (28, 50).

In iron mound systems (16, 59) that contain abundant Fe(III), greigite formation is likely to be diminished. In this context, the Fe(III)RB- and SRB-induced schwertmannite-to-goethite transformation will exert significant control on the geochemistry of AMD-impacted systems. FeOB activities in iron mounds, while oxidatively precipitating Fe, lead to further acidification of AMD, enhancing the solubility of Fe^{3+} and limiting the effectiveness of Fe removal. Anaerobic activities may enhance the stability of Fe(III) phases after they have been precipitated in iron mound systems. Goethite is less soluble than schwertmannite (log solubility product [K_{sp}] = 1.4 and 18, respectively [6, 48]), rendering it less susceptible to dissolution under acidic conditions. Furthermore, since goethite is a less thermodynamically favorable TEA in comparison to schwertmannite (equations 5 and 6), the microbially mediated transformation of schwertmannite to goethite would render the goethite-associated pool of Fe(III) more resistant to further microbial reduction and consequently, enhance the stability of Fe(III). Despite the potential for reductive rerelease of Fe resulting from SRB activities in iron mound systems, it appears the SRB activities may enhance the stability of Fe after it has been oxidatively immobilized in iron mound systems.

ACKNOWLEDGMENTS

This work was supported by a Faculty Research Grant (FRG) and start-up funds provided by the University of Akron (J.M.S.).

REFERENCES

1. **Alazard D, Manon J, Battaglia-Brunet F, Cayol J-L, Ollivier B.** 2010. *Desulfosporosinus acidiphilus* sp. nov.: a moderately acidophilic sulfate-reducing bacterium isolated from acid mining drainage sediments. Extremophiles **14**:305–312.
2. **Baker BJ, Banfield JF.** 2003. Microbial communities in acid mine drainage. FEMS Microbiol. Ecol. **44**:139–152.
3. **Bazylinski DA, Moskowitz BM.** 1997. Microbial biomineralization of magnetic minerals: microbiology, magnetism, and environmental significance. Rev. Mineral. **35**:181–223.
4. **Benner SG, Blowes DW, Ptacek CJ, Mayer KU.** 2002. Rates of sulfate reducing and metal sulfide precipitation in a permeable reactive barrier. Appl. Geochem. **17**:301–320.
5. **Bigham JM, Schwertmann U, Pfab G.** 1996. Influence of pH on mineral speciation in a bioreactor simulating acid mine drainage. Appl. Geochem. **11**:845–849.
6. **Bigham JM, Schwertmann U, Traina SJ, Winland RL, Wolf M.** 1996. Schwertmannite and the chemical modeling of iron in acid sulfate waters. Geochim. Cosmochim. Acta **60**:2111–2121.
7. **Blöthe M, et al.** 2008. pH gradient-induced heterogeneity of Fe(III)-reducing microorganisms in coal mining-associated lake sediments. Appl. Environ. Microbiol. **74**:1019–1029.
8. **Bozau E, et al.** 2007. Biotechnological remediation of an acidic pit lake: modeling the basic processes in a mesocosm experiment. J. Geochem. Explor. **92**:212–221.
9. **Burton ED, Bush RT, Sullivan LA, Mitchell DRG.** 2007. Reductive transformations of iron and sulfur in schwertmannite-rich accumulations associated with acidified coastal lowlands. Geochim. Cosmochim. Acta **71**:4456–4473.
10. **Burton ED, Bush RT, Sullivan LA, Mitchell DRG.** 2008. Schwertmannite transformation to goethite via the Fe(II) pathway: reaction rates and implications for iron-sulfide formation. Geochim. Cosmochim. Acta **72**: 4551–4564.
11. **Burton ED, et al.** 2010. Arsenic effects and behavior in association with the Fe(II)-catalyzed transformation of schwertmannite. Environ. Sci. Technol. **44**:2016–2021.
12. **Cline JD.** 1969. Spectrophotometric determination of hydrogen sulfide in natural waters. Limnol. Oceanogr. **14**:454–458.
13. **Coupland K, Johnson DB.** 2008. Evidence that the potential for dissimilatory ferric iron reduction is widespread among acidophilic heterotrophic bacteria. FEMS Microbiol. Lett. **279**:30–35.
14. **Cravotta CA, III.** 2003. Size and performance of anoxic limestone drains to neutralize acidic mine drainage. J. Environ. Qual. **32**:1277–1289.
15. **Dean JA.** 1985. Lange's handbook of chemistry, 13th ed. McGraw-Hill, New York, NY.
16. **DeSa TC, Brown JF, Burgos WD.** 2010. Laboratory and field-scale evaluation of low-pH Fe(II) oxidation at Hughes Borehole, Portage, Pennsylvania. Mine Water Environ. **29**:239–247.
17. **dos Santos Afonso M, Stumm W.** 1992. Reductive dissolution of iron(III) (hydr)oxides by hydrogen sulfide. Langmuir **8**:1671–1675.
18. **Downs RT, Hall-Wallace M.** 2003. The American Mineralogist Crystal Structure Database. Am. Mineral. **88**:247–250.
19. **Dunlop DJ, Ö. Özdemir.** 1997. Rock magnetism. Cambridge University Press, New York, NY.
20. **Evans ME, Heller F.** 2003. Environmental magnetism: principles and applications of environmagnetics. Academic Press, New York, NY.
21. **Fortin D, Rioux J-P, Roy M.** 2002. Geochemistry of iron and sulfur in the zone of microbial sulfate reduction in mine tailings. Water Air Soil Pollut. **2**:37–56.
22. **Geller W, et al.** 2008. A pilot-scale field experiment for the microbial neutralization of holomictic acidic pit lake. J. Geochem. Explor. **100**: 153–159.
23. **González-Toril E, Aquilera Á, Souza-Egipsy V, Pamo EL, España JS, Amils R.** 2011. Geomicrobiology of La Zarza-Perrunal acid mine effluent (Iberian Pyrite Belt, Spain). Appl. Environ. Microbiol. **77**:2685–2694.
24. **Gramp JP, Bigham JM, Jones FS, Tuovinen OH.** 2010. Formation of Fe-sulfides in cultures of sulfate-reducing bacteria. J. Hazard. Mater. **175**: 1062–1067.
25. **Herbert RB, Jr, Benner SG, Pratt AR, Blowes DW.** 1998. Surface chemistry and morphology of poorly crystalline iron sulfides precipitated in media containing sulfate reducing bacteria. Chem. Geol. **144**:87–97.
26. **Herlihy AT, Kaufmann PR, Mitch ME.** 1990. Regional estimates of acid mine drainage impact on streams in the Mid-Atlantic and Southeastern United States. Water Air Soil Pollut. **50**:91–107.
27. **Hiibel SR, et al.** 2008. Microbial community analysis of two field-scale sulfate-reducing bioreactors treating mine drainage. Environ. Microbiol. **10**:2087–2097.
28. **Johnson DB, Hallberg KB.** 2002. Pitfalls of passive mine water treatment. Rev. Environ. Sci. Biotechnol. **1**:335–343.
29. **Johnson DB, Hallberg KB.** 2009. Carbon, iron and sulfur metabolism in acidophilic micro-organisms. Adv. Microb. Physiol. **54**:201–255.
30. **Jönsson J, Persson P, Sjöberg S, Lövgren L.** 2005. Schwertmannite precipitated from acid mine drainage: phase transformation, sulfate release and surface properties. Appl. Geochem. **20**:179–191.
31. **Knorr K-H, Blodau C.** 2007. Controls on schwertmannite transformation rates and products. Appl. Geochem. **22**:2006–2015.
32. **Koschorreck M, et al.** 2010. Structure and function of the microbial community in an *in situ* reactor to treat an acidic mine pit lake. FEMS Microbiol. Ecol. **73**:385–395.
33. **Lee Y-J, Romanek CS, Wiegel J.** 2009. *Desulfosporosinus youngiae* sp. nov., a spore-forming, sulfate-reducing bacterium isolated from a constructed wetland treating acid mine drainage. Int. J. Syst. Evol. Microbiol. **59**:2743–2746.
34. **Lennie AR, et al.** 1997. Transformation of mackinawite to greigite: an in situ X-ray powder diffraction and transmission electron microscopy study. Am. Mineral. **82**:302–309.
35. **Lovley DR, Phillips EJP.** 1987. Rapid assay for microbially reducible ferric iron in aquatic sediments. Appl. Environ. Microbiol. **53**:1536–1540.
36. **Lu S, et al.** 2010. Ecophysiology of Fe-cycling bacteria in acidic sediments. Appl. Environ. Microbiol. **76**:8174–8183.
37. **Majzlan J, et al.** 2003. Thermodynamics of Fe oxides: Part I. Entropy at standard temperature and pressure and heat capacity of goethite (α-FeOOH), lepidocrocite (γ-FeOOH), and maghemite (γFe_2O_3). Am. Mineral. **88**:846–854.
38. **Marius MS, James PAB, Bahaj AS, Smallman DJ.** 2005. Influence of iron valency on the magnetic susceptibility of a microbially produced iron sulphide. J. Phys. Conf. Ser. **17**:65–69.
39. **Neal AL, et al.** 2001. Iron sulfides and sulfur species produced at hematite surfaces in the presence of sulfate-reducing bacteria. Geochim. Cosmochim. Acta **65**:223–235.
40. **Peretyazhko T, et al.** 2009. Mineralogical transformations controlling acid mine drainage chemistry. Chem. Geol. **262**:169–178.
41. **Porsch K, Meier K, Kleinsteuber S, Wendt-Potthoff K.** 2009. Importance of different physiological groups of iron reducing microorganisms in an acidic mining lake remediation experiment. Microb. Ecol. **57**: 701–717.
42. **Porsch K, Dippon U, Rijal ML, Appel E, Kappler A.** 2010. In-situ magnetic susceptibility measurements as a tool to follow geomicrobiological transformation of Fe minerals. Environ. Sci. Technol. **44**:3846–3852.
43. **Pósfai M, Busceck PR, Frankel RB, Bazylinski DA.** 1998. Reaction sequence of iron sulfide minerals in bacteria and their use as biomarkers. Science **280**:880–883.
44. **Pósfai P, Busceck MPR, Bazylinski DA, Frankel RB.** 1998. Iron sulfides from magnetotactic bacteria: structure, composition, and phase transitions. Am. Mineral. **83**:1469–1481.
45. **Postma D, Jakobsen R.** 1996. Redox zonation: equilibrium constraints on the Fe(III)/SO_4-reduction interface. Geochim. Cosmochim. Acta **60**: 3169–3175.
46. **Poulton SW, Krom MD, Raiswell R.** 2004. A revised scheme for the reactivity of iron (oxyhydr)oxide minerals towards dissolved sulfide. Geochim. Cosmochim. Acta **68**:3703–3715.
47. **Ramamoorthy S, et al.** 2006. *Desulfosporosinus lacus* sp. nov., a sulfate-reducing bacterium isolated from pristine freshwater lake sediments. Int. J. Syst. Evol. Microbiol. **56**:2729–2736.
48. **Regenspurg S, Brand A, Peiffer S.** 2004. Formation and stability of schwertmannite in acidic mining lakes. Geochim. Cosmochim. Acta **68**: 1185–1197.
49. **Rickard DT.** 1969. The microbiological formation of iron sulphides. Stockholm Contrib. Geol. **20**:50–66.
50. **Rickard D, Luther GW, III.** 2007. Chemistry of iron sulfides. Chem. Rev. **107**:514–562.
51. **Roberts AP, et al.** 2006. Characterization of hematite (α-Fe_2O_3), goethite (α-FeOOH), greigite (Fe_3S_4), and pyrrohotite (Fe_7S_8) using first order reversal curve diagrams. J. Geophys. Res. **111**:B12S35.
52. **Roberts AP, Weaver R.** 2005. Multiple mechanisms of remagnetization

involving sedimentary greigite (Fe_7S_8). Earth Planet. Sci. Lett. **231**: 263–277.
53. **Robertson WJ, Bowmann JP, Franzmann PD, Mee BJ.** 2001. *Desulfosporosinus meridiei* sp. nov., a spore-forming sulfate-reducing bacterium isolated from gasoline-contaminated groundwater. Int. J. Syst. Evol. Microbiol. **51**:133–140.
54. **Rouchette P, et al.** 2005. Non-saturation of the defect moment of goethite and fine grained hematite up to 57 Teslas. Geophys. Res. Lett. **32**:L22309.
55. **Sánchez-Andrea I, Rodríguez N, Amils R, Sanz JL.** 2011. Microbial diversity in anaerobic sediments at Río Tinto, a naturally acidic environment with a high heavy metal content. Appl. Environ. Microbiol. **77**: 6085–6093.
56. **Schoonen MAA, Barnes HL.** 1991. Reactions forming pyrite and marcasite from solution. II. Via FeS precursors below 100°C. Geochim. Cosmochim. Acta **55**:1505–1514.
57. **Schwertmann U, Carlson L.** 2005. The pH-dependent transformation of schwertmannite to goethite at 25°C. Clay Minerals **40**:63–66.
58. **Senko JM, Bertel D, Quick TJ, Burgos WD.** 2011. The influence of phototrophic biomass on Fe and S redox cycling in an acid mine drainage-impacted system. Mine Water Environ. **30**:38–46.
59. **Senko JM, Wanjugi P, Lucas M, Bruns MA, Burgos WD.** 2008. Characterization of Fe(II) oxidizing bacterial activities and communities at two acidic Appalachian coal mine drainage-impacted sites. ISME J. **2**:1134–1145.
60. **Senko JM, Zhang G, McDonough JT, Bruns MA, Burgos WD.** 2009. Metal reduction at low pH by a *Desulfosporosinus* species: implications for the biological treatment of acid mine drainage. Geomicrobiol. J. **26**:71–82.
61. **Snowball I, Torri M.** 1999. Incidence and significance of ferrimagnetic iron sulphides in quaternary studies, p 199–230. *In* Maher BA, Thompson R (ed), Quaternary climates, environments and magnetism. Cambridge University Press, New York, NY.
62. **Stackebrandt E, Schumann P, Schüler E, Hippe H.** 2003. Reclassification of *Desulfotomaculum auripigmentum* as *Desulfosporosinus auripigmenti* corrig., comb. nov. Int. J. Syst. Evol. Microbiol. **53**:1439–1443.
63. **Stookey LL.** 1970. Ferrozine-a new spectrophotometric reagent for iron. Anal. Chem. **42**:779–781.
64. **Tanner RS.** 1997. Cultivation of bacteria and fungi, p 52–60. *In* Hurst CJ, Knudsen GR, McInerney MJ, Stetzenbach LD, Walter MV (ed), Manual of environmental microbiology. ASM Press, Washington, DC.
65. **Vatsurina A, Badrutdinova D, Schumann P, Spring S, Vainshtein M.** 2008. *Desulfosporosinus hippie* sp. nov., a mesophilic sulfate-reducing bacterium isolated from permafrost. Int. J. Syst. Evol. Microbiol. **58**: 1228–1232.
66. **Watson JHP, et al.** 1995. Heavy metal adsorption on bacterially produced FeS. Mineral Eng. **8**:1097–1108.
67. **Wilkin RT, Barnes HL.** 1997. Formation process of framboidal pyrite. Geochim. Cosmochim. Acta **61**:323–339.
68. **Winch S, Mills HJ, Kostka JE, Fortin D, Lean DRS.** 2009. Identification of sulfate-reducing bacteria in methylmercury-contaminated mine tailings by analysis of SSU rRNA genes. FEMS Microbiol. Ecol. **68**:94–107.
69. **Winklhofer M, Zimanyi GT.** 2006. Extracting the intrinsic switching field distribution in perpendicular media: a comparative analysis. J. Appl. Phys. **99**:08E710.